A Revised Wigner Function Approach for Stationary Quantum Transport

Robert Kosik$^{(\boxtimes)}$, Johann Cervenka, Mischa Thesberg, and Hans Kosina

Institute for Microelectronics, TU Wien, Vienna, Austria
{kosik,cervenka,thesberg,kosina}@iue.tuwien.ac.at
http://www.iue.tuwien.ac.at

Abstract. The Wigner equation describing stationary quantum transport has a singularity at the point $k = 0$. Deterministic solution methods usually deal with the singularity by just avoiding that point in the mesh (e.g., Frensley's method). Results from such methods are known to depend strongly on the discretization and meshing parameters.

We propose a revised approach which explicitly includes the point $k = 0$ in the mesh. For this we give two equations for $k = 0$. The first condition is an algebraic constraint which ensures that the solution of the Wigner equation has no singularity for $k = 0$. If this condition is fulfilled we then can derive a transport equation for $k = 0$ as a secondary equation.

The resulting system with two equations for $k = 0$ is overdetermined and we call it the constrained Wigner equation. We give a theoretical analysis of the overdeterminacy by relating the two equations for $k = 0$ to boundary conditions for the sigma equation, which is the inverse Fourier transform of the Wigner equation.

We show results from a prototype implementation of the constrained equation which gives good agreement with results from the quantum transmitting boundary method. No numerical parameter fitting is needed.

Keywords: Wigner function · Sigma function · Finite difference method · Constrained equation · Quantum transport · Device simulation · Resonant tunneling diode

1 Wigner Function Formalism

An attractive approach to quantum transport simulation is based on the Wigner function formulation of quantum mechanics [8] because it is formally close to a classical phase space description and allows one to use a mixed quantum-classical description of the system. This work deals with the stationary Wigner equation in a single spatial dimension.

1.1   Wigner Function

The Wigner function $f(r, k)$ is derived from the von Neumann density function $\rho(x, y)$ as the result of two consecutive transformations.

1. Introduce new coordinates for the quantum density

$$r = \frac{x + y}{2}, \qquad s = x - y.$$

   Using these coordinates the density matrix transforms into an intermediate form, which we call the sigma function

$$\sigma(r, s) = \rho(r + \frac{s}{2}, r - \frac{s}{2}). \tag{1}$$

2. The Wigner function $f(r, k)$ is derived from the sigma function $\sigma(r, s)$ via a Fourier transform in coordinate s

$$f(r, k) = \frac{1}{2\pi} \int \sigma(r, s)\, e^{-i\,k\,s}\, ds. \tag{2}$$

With these conventions a Schrödinger plane wave $\psi = e^{ik_0 x}$ has a corresponding sigma function $e^{ik_0 s}$ and a Wigner function $\delta(k - k_0)$.

1.2   Wigner Equation

Stationary quantum transport is described by the Liouville-von Neumann equation for the density matrix $\rho(x, y)$

$$-\frac{\hbar^2}{2m} \left(\frac{\partial^2}{\partial x^2} - \frac{\partial^2}{\partial y^2} \right) \rho + \big(V(x) - V(y)\big)\rho = 0 \tag{3}$$

where $V(x)$ is the potential energy. Using coordinates (r, s) the stationary von Neumann equation transforms into the stationary sigma equation

$$\frac{\hbar^2}{m} \frac{\partial^2 \sigma}{\partial rs} = U(r, s)\sigma(r, s) \tag{4}$$

where the potential term $U(r, s)$ is defined by

$$U(r, s) = V\left(r + \frac{s}{2}\right) - V\left(r - \frac{s}{2}\right). \tag{5}$$

In a single spatial dimension equation (4) is the characteristic hyperbolic form of the stationary von Neumann equation (3).

Applying the Fourier transform (2) to the sigma equation (4) gives the stationary Wigner equation

$$\frac{\hbar k}{m} \frac{\partial f(r, k)}{\partial r} = \int f(r, k - k')V_w(r, k')dk'. \tag{6}$$

Here the Wigner potential $V_w(r, k)$ is defined as the Fourier transform of $U(r, s)$ divided by $i\hbar$

$$V_w(r, k) = \frac{1}{i\hbar} \frac{1}{2\pi} \int U(r, s) e^{-iks} ds. \tag{7}$$

For non-zero bias the Wigner potential has a $1/k$-singularity at $k = 0$.

For open systems classical inflow boundary conditions (BCs) are imposed on the stationary Wigner equation (two-point boundary value problem)

$$f(r_{min}, k) = f_L(k) \quad \text{(for } k > 0) \qquad\qquad f(r_{max}, k) = f_R(k) \quad \text{(for } k < 0). \tag{8}$$

Here f_L and f_R are prescribed distributions depending on temperature and the doping concentration in the electrodes.

2   Critique of Frensley's Method

In a single space the Wigner equation (6) can be rewritten for $k \neq 0$ as

$$\frac{\partial f(r, k)}{\partial r} = \frac{1}{k} \frac{m}{\hbar} \int f(r, k - k') V_w(r, k') dk'. \tag{9}$$

The form (9) emphasizes that the equation becomes singular at $k = 0$.

In [3] William Frensley proposed a discrete method for the Wigner equation (9). A special feature of the method is that it uses an equi-spaced grid shifted by $\triangle k/2$ excluding the point $k = 0$. Frensley's original discretization solves the Wigner equation (9) using upwinding on a coarse r-grid.

However, the method has been criticized for the results depending strongly on the type of discretization used and its parameters. The upwinding introduces a lot of artificial diffusion and the method breaks down when the grid is refined.

Figure 1 displays numerical results from the simulation of Tsuchiya's resonant tunneling diode [7]. All results were calculated using shooting methods and massive parallelization. The coherence length is kept fixed in this example (fixed k-grid). With refinement of $\triangle r$ the artificial diffusion is reduced and simulation results using upwinding slowly converge to the numerically exact solution (semi-discrete solution). The upper solid red line was calculated without upwinding using $N_r = 800$ points. It does not change noticeably if the r-grid is refined.

3   Constrained Wigner Equation

Unfortunately, the numerically exact solution appears to be unphysical, showing no negative differential resistance and too high current. Furthermore, on close inspection, numerical solutions $f(r, k)$ show a sharp discontinuity and strong negative values around $k = 0$.

Theoretical analysis motivated by these observations lead to the insight that the breakdown is due to the inadequate treatment of the equation near the singular point $k = 0$.

If we want to avoid a singularity we actually get two equations for $k = 0$ and thus an overdetermined system:
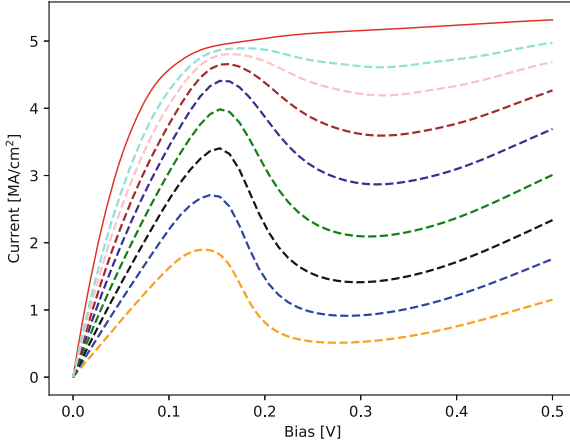
Fig. 1. The dashed lines are I–V curves from Frensley's discretization using upwinding with $N_r = 800$ (orange), $N_r = 1600$ (blue), all the way up to $N_r = 102400$ (cyan). With refinement the dashed lines slowly converge towards the upper solid red line which is the solution without upwinding. (Color figure online)

1. Putting $k = 0$ in (6) gives the following regularity constraint

$$\int f(r, k')V_w(r, k')dk' = 0. \tag{10}$$

In this degenerate case the left hand side in Eq. (6) vanishes and we do not get a differential equation. This special case is called an algebraic constraint in [1,5]. It is needed to avoid poles on the right hand side of (9). The regularity constraint has also a physical interpretation: The total inscattering rate at $k = 0$ must vanish in the steady state.

2. If constraint (10) is fulfilled then (using L'Hospital's rule for a quotient and Leibniz's rule for differentiation under the integral sign) we can take the limit $k \to 0$ in (9). This gives the "transport" equation at $k = 0$

$$\frac{\partial f(r,0)}{\partial r} = \frac{m}{\hbar} \int f_k(r, -k')V_w(r, k')dk' = -\frac{m}{\hbar} \int f_k(r, k')V_w(r, k')dk'. \tag{11}$$

Here $f_k(r, k) = \frac{\partial f(r,k)}{\partial k}$ denotes the first order k-derivative of $f(r, k)$.

We call the overdetermined system with two equations for $k = 0$ the constrained Wigner equation.

It has to be pointed out, that the zero bias case is special. In this case the Wigner potential is not singular at $k = 0$ and the ansatz $\tilde{f}(r, k) = \frac{h(r,k)}{k}$ gives a well-defined equation for h. The solution $\tilde{f}$ has a pole at $k = 0$ and the regularity constraint (10) is not necessarily fulfilled. In addition, for zero bias the solution may contain contributions $g(r)\delta(k)$.

4   Constrained Sigma Equation

The significance of a parallel investigation of the sigma equation and the Wigner equation is explained by noting that the two equations for $k = 0$ are related to two types of boundary conditions for the sigma function. A constrained sigma equation corresponding to the constrained Wigner equation is derived in this section.

4.1   Goursat Problem

The sigma function has the symmetry property $\sigma(r, -s) = \overline{\sigma(r, s)}$. Its real part is even, the imaginary part b is an odd function in s. This allows one to define a purely real sigma function $\tilde{\sigma}$

$$\tilde{\sigma}(r, s) = a(r, s) + b(r, s) \tag{12}$$

which is useful to avoid complex numbers in the numerical implementation and for visualization. The function $\tilde{\sigma}$ is a real solution to the sigma equation (4).

Integrating both sides of (4) over a rectangular domain gives

$$\sigma(r, s) = \sigma_0(r, s) + \int_0^r \int_0^s \frac{m}{\hbar^2} U(r', s') \sigma(r', s') \, dr' \, ds' \tag{13}$$

where $\sigma_0(r, s)$ is a solution to the homogeneous sigma equation. A homogeneous solution σ_0 is of the form

$$\sigma_0(r, s) = \phi(r) + \psi(s) - \phi(0), \qquad \phi(0) = \psi(0). \tag{14}$$

The solution σ of (13) fulfills $\sigma(0, s) = \psi(s)$ and $\sigma(r, 0) = \phi(r)$, which are boundary conditions of Goursat type. In general, these consist in boundary conditions on an angle formed by two characteristics. Equation (13) is a two-dimensional integral equation of Volterra type. Existence and uniqueness of the solution to the Goursat problem can be proved [2,6].

Note that inflow boundary conditions as defined in Eq. (8) for the Wigner equation can also be imposed in the sigma equation by calculating the Fourier transform of the sigma function on the boundary s-lines at r_{min}, r_{max}.

In contrast to the Wigner equation, the sigma equation has an additional freedom in the choice of boundary conditions, because boundary conditions $\phi(r)$ on a characteristic r-line have no immediate analogue in the Wigner equation.

4.2   BCs for the Constrained Sigma Equation

The two equations for $k = 0$ in the constrained Wigner equation can be related to boundary conditions for the sigma equation.

Regularity Constraint: Periodic BCs. The regularity constraint is the Wigner equation for $k = 0$. In s-space the regularity constraint (10) becomes

$$\int_{-a}^{a} U(r,s)\sigma(r,s)ds = 0 \tag{15}$$

assuming a symmetric finite s-interval $(-a, a)$. Integrating both sides of the sigma equation (4) over the interval $(-a, a)$ we derive

$$\sigma_r(a) - \sigma_r(-a) = \frac{m}{\hbar^2} \int_{-a}^{a} U(r,s)\sigma(r,s)ds = 0 \tag{16}$$

and hence constraint (15) is related to periodic BCs for σ_r on a symmetric, finite domain.

Transport Equation at $k = 0$: Anti-periodic BCs. To study the transport equation at $k = 0$ in the sigma representation we take the inverse Fourier transform of Eq. (11) which gives

$$\int \frac{\partial \sigma(r,s)}{\partial r} ds = -\frac{m}{\hbar^2} \int s\, U(r,s)\sigma(r,s)ds. \tag{17}$$

Multiplying the stationary sigma equation (4) with $-s$ and integrating over s gives

$$-\int s \frac{\partial}{\partial r} \frac{\partial}{\partial s} \sigma(r,s)ds = -\frac{m}{\hbar^2} \int s\, U(r,s)\sigma(r,s)ds. \tag{18}$$

Subtracting the two Eqs. (17) and (18) we get a condition on σ_r which is independent of U

$$\int \frac{\partial}{\partial s}[s \frac{\partial}{\partial r}\sigma(r,s)]ds = 0. \tag{19}$$

On a finite symmetric domain this gives anti-periodic boundary conditions for σ_r, i.e., $\sigma_r(r, -a) = -\sigma_r(r, a)$. The sigma equation with anti-periodic BCs for σ in s-space is related to Frensley's method which uses a shifted k-grid.

Overdetermined Boundary Value Problem. Summarizing we have both periodic and anti-periodic boundary conditions for σ_r. It follows that $\sigma_r = 0$ and σ is constant on the s-boundaries. The only reasonable choice for the integration constant is to set

$$\sigma(r, s_{max}) = \sigma(r, s_{min}) = 0 \tag{20}$$

on a s-domain symmetric around $s = 0$.

The constrained sigma equation consists of double homogeneous boundary conditions (20) plus inflow boundary conditions imposed on the Fourier transform of σ. This system is also overdetermined and corresponds to the constrained Wigner equation.

5   Proof of Concept

Results from a prototype implementation are included down below. This should serve as a proof of concept and back up our claims about the root cause of numerical problems and inconsistencies, which are observed in stationary simulations based on Frensley's method.

The version easiest to implement has been chosen for prototyping. It uses double homogeneous boundary conditions in the sigma equation. We use an orthogrid and a stencil

$$\sigma(0,0) + \sigma(1,1) - \sigma(0,1) - \sigma(1,0) \;=\; \frac{1}{4} \sum_{i=0}^{1} \sum_{j=0}^{1} \tilde{U}(i,j)\sigma(i,j) \qquad (21)$$

for the unit square.

Using Lagrange multipliers, inflow boundary conditions are fulfilled exactly and conservation of mass is also exact. The remaining equations of the overdetermined system are only fulfilled approximately. A sparse direct solver is used for the least squares solution of the system.

For a test we simulated a GaAs-AlGaAs double barrier resonant tunneling diode (barrier width 2.8 nm, well width 4.5 nm) as specified in [7]. The coherence length used in the simulation is 36 nm. The simulation is done for two grid sizes. The dotted line is the result for $(N_r = 500, N_s = 400)$. The grid is then refined once in each dimension. The dashed line is the result for $(N_r = 1000, N_s = 800)$. As seen in Fig. 2 the solution from the constrained sigma equation changes
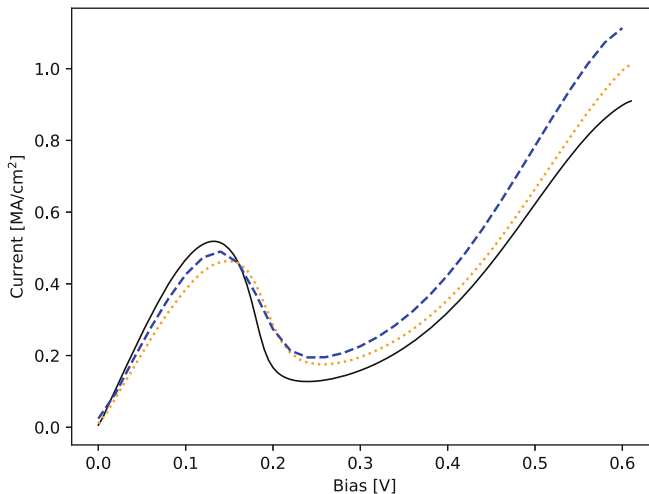
Fig. 2. The solid line is the solution from the QTBM, which is compared with the two solutions from the constrained sigma equation for $N_r = 500$ (dotted) and $N_r = 1000$ (dashed). The resonance from the QTBM is reproduced. No parameter fitting is employed. The method is stable under mesh refinement.

with the refinement but it is quite stable. This should be compared with grid refinement for Frensley's method in Fig. 1. As we cannot use a shooting method for the constrained equation, the use of very fine meshes like in Fig. 1 (up to $N_r = 102400$) is not computationally feasible.

In the same figure the two constrained solutions are compared with the result from the quantum transmitting boundary method (QTBM) [4]. The fit with the QTBM (solid line) is reasonably good for the resonance peak. At higher bias we get a discrepancy, which needs further research.

For non-zero bias, the Wigner transforms of the scattering modes assumed in the QTBM are solutions to the constrained Wigner equation. However, the Wigner function model assumes classical boundary conditions and a finite coherence length, hence a perfect fit with QTBM is not to be expected.

In contrast to the results from Frensley's method (see Fig. 1), the results from the constrained Wigner equation are physically reasonable and consistent when the grid is refined. We believe that initial results for the constrained equation as demonstrated in Fig. 2 are encouraging and that the revised method deserves further in-depth study.

References

1. Arnold, A., Lange, H., Zweifel, P.F.: A discrete-velocity, stationary Wigner equation. J. Math. Phys. **41**(11), 7167–7180 (2000). https://doi.org/10.1063/1.1318732
2. Brunner, H.: Collocation Methods for Volterra Integral and Related Functional Equations. Cambridge University Press, Cambridge (2004). https://doi.org/10.1017/cbo9780511543234
3. Frensley, W.R.: Boundary conditions for open quantum systems driven far from equilibrium. Rev. Mod. Phys. **62**(3), 745–791 (1990). https://doi.org/10.1103/RevModPhys.62.745
4. Lent, C.S., Kirkner, D.: The quantum transmitting boundary method. J. Appl. Phys. **67**(10), 6353–6359 (1990). https://doi.org/10.1063/1.345156
5. Li, R., Lu, T., Sun, Z.: Parity-decomposition and moment analysis for stationary Wigner equation with inflow boundary conditions. Front. Math. China **12**(4), 907–919 (2017). https://doi.org/10.1007/s11464-017-0612-9
6. Suryanarayana, M.B.: On multidimensional integral equations of Volterra type. Pac. J. Math. **41**(3), 809–828 (1972). https://doi.org/10.2140/pjm.1972.41.809
7. Tsuchiya, H., Ogawa, M., Miyoshi, T.: Simulation of quantum transport in quantum devices with spatially varying effective mass. IEEE Trans. Electron Devices **38**(6), 1246–1252 (1991). https://doi.org/10.1109/16.81613
8. Wigner, E.P.: On the quantum correction for thermodynamic equilibrium. Phys. Rev. **40**(5), 749–759 (1932). https://doi.org/10.1103/PhysRev.40.749